Struct Multidisc Optim (2008) 36:59–70
DOI 10.1007/s00158-007-0200-9

RESEARCH PAPER

Aero-structural optimization using adjoint coupled post-optimality sensitivities

Ian R. Chittick · Joaquim R. R. A. Martins

Received: 8 May 2007 / Revised: 5 September 2007 / Accepted: 9 October 2007 / Published online: 13 December 2007

Abstract A new subspace optimization method for performing aero-structural design is introduced. The method relies on a semi-analytic adjoint approach to the sensitivity analysis that includes post-optimality sensitivity information from the structural optimization subproblem. The resulting coupled post-optimality sensitivity approach is used to guide a gradient-based optimization algorithm. The new approach simplifies the system-level problem, thereby reducing the number of calls to a potentially costly aerodynamics solver. The aero-structural optimization of an aircraft wing is performed using linear aerodynamic and structural analyses, and a performance comparison is made between the new approach and the conventional multidisciplinary feasible method. The new asymmetric suboptimization method is found to be the more efficient approach when it adequately reduces the number of system evaluations or when there is a large enough discrepancy between disciplinary solution times.

Keywords Aero-structural optimization · Subspace optimization · Asymmetric suboptimization · Coupled post-optimality sensitivity analysis · Coupled-adjoint sensitivity analysis

I. R. Chittick (✉) · J. R. R. A. Martins
University of Toronto Institute for Aerospace Studies, 4925 Dufferin Street, Toronto, ON M3H 5T6, Canada
e-mail: ian.chittick@utoronto.ca

J. R. R. A. Martins
e-mail: martins@utias.utoronto.ca

1 Introduction

1.1 MDO architectures

Extensive research has been conducted in the field of multidisciplinary design optimization (MDO) and its application to aircraft design. The survey paper by Sobieszczanski-Sobieski and Haftka (1997) provides a comprehensive overview of the work accomplished in this area, highlighting the different strategies that have been inspired by the inherent challenges of MDO. One of the most common applications of MDO techniques is coupled aerodynamic and structural (aero-structural) optimization, because the interaction between these two disciplines is a primary consideration in the design of aircraft.

The interdisciplinary coupling intrinsic to MDO tends to pose significant organizational and computational challenges, and there exist several different MDO architectures for dealing with this complexity, as compared by Tedford and Martins (2006). These architectures can be divided into two main classes: single-level formulations and multilevel formulations. Single-level formulations, such as the multidisciplinary feasible (MDF) and the individual discipline feasible architectures, impose a single, system-level optimizer that is given control over the entire state of the system (Cramer et al. 1994; Tribes et al. 2005). Multilevel formulations, which include collaborative optimization (Kroo 1997; Braun et al. 1996) and bi-level integrated system synthesis (BLISS; Sobieszczanski-Sobieski et al. 1998; Kodiyalam and Sobieszczanski-Sobieski 2002), divide the original problem into smaller subproblem optimizations.

In this research, we develop a new hybrid architecture that involves a subspace optimization. The objective is to decrease the cost of solving MDO problems that exhibit a large discrepancy between disciplinary solution times, as is often the case in high-fidelity aero-structural optimization (Martins et al. 2004). The crucial consideration for good convergence properties is the efficient computation of multidisciplinary sensitivities. To accomplish this, the coupled adjoint method (Martins et al. 2005) is expanded to include post-optimality information from the subspace optimization.

1.2 Motivation

The trade-off between drag and structural weight for aircraft wings is governed by two main interactions between the aerodynamics and structures. First, the structural weight affects the required lift, which in turn affects the lift-induced drag. Second, the aerodynamic loads affect the structural deformations, which in turn change the aerodynamic shape. Therefore, to obtain a converged aero-structural state, several iterations of the two disciplines are needed.

Different researchers have addressed the challenge of performing high-fidelity aero-structural analysis and optimization (Maute et al. 2001; Giunta 2000; Chattopadhyay and Pagaldipti 1995). However, due to the high computational costs involved, practical implementations have generally been limited to only a few design variables. The key to solving such large optimization problems was the development of the coupled adjoint equations, which made it possible to efficiently compute gradients with respect to large numbers of design variables (Martins et al. 2005). Since then, several observations were made that resulted in new research directions. For instance, to take advantage of the adjoint approach, new ways to aggregate stress constraints were developed by Poon and Martins (2007). Another issue was the fact that the computational cost of the aerodynamic analysis, which involves a computational fluid dynamics solver, was an order of magnitude greater than the structural analysis (a linear finite-element solver).

The goal of the present work is to take advantage of this computational imbalance by solving a structural subspace optimization problem within the aero-structural analysis module. The conventional MDF approach is shown in Fig. 1 along with the proposed architecture in Fig. 2. Throughout this paper, the routine that converges a coupled set of disciplines will be referred to as the multidisciplinary analysis (MDA) module. Therefore, the MDA in the MDF method involves the aerodynamic and structural analyses, whereas the

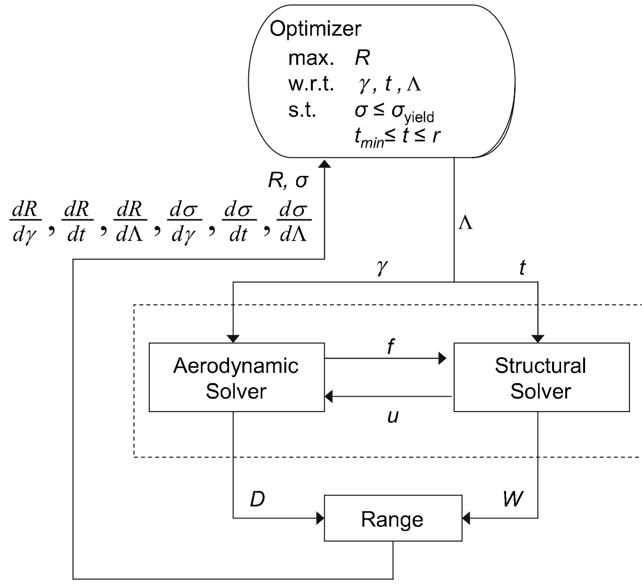

Fig. 1 MDF formulation

MDA in the new method includes the aerodynamic analysis and the structural suboptimization. The presence of the subspace optimization in the proposed architecture means that, for each aerodynamic analysis, one has to perform a structural optimization, which will increase the computational cost of the MDA. The advantage of this asymmetric suboptimization method, however, is that it simplifies the system-level problem by relocating all of the structural design variables and constraints within the structural discipline. This reduces the amount of gradient information required by the system-level optimizer and should decrease the num-

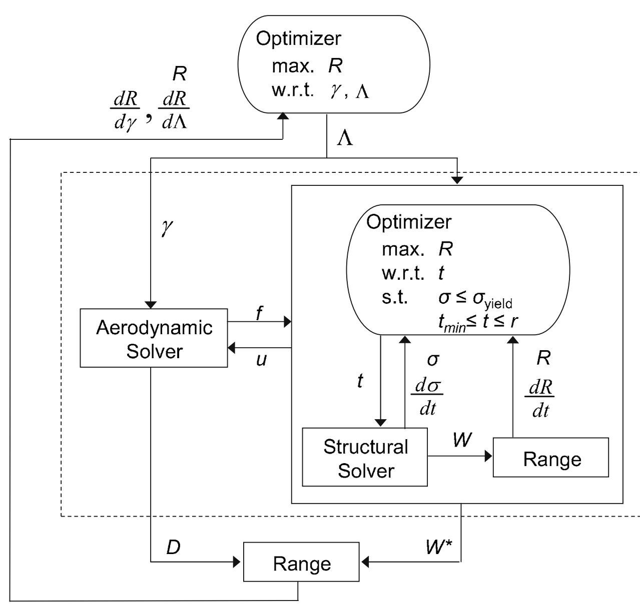

Fig. 2 Proposed asymmetric suboptimization method

ber of calls to the costly aerodynamic analysis. This is accomplished without having to compromise the influence of the structures on the aerodynamics. The interactions between the disciplines are modeled exactly, and the fidelity of the analyses is not limited by any approximation technique, such as a response surface, which are sometimes used in hierarchical architectures (Sobieski and Kroo 2000).

1.3 Architecture implementation

Motivation for the asymmetric suboptimization method originated from the discrepancy in disciplinary solution times apparent in fluid-structure interactions. However, the concept behind the new formulation is not limited to aero-structural optimization or even to systems with only two participating disciplines. Therefore, the implementation details of the new method will be described using general notation to account for larger and more complex design applications.

The following discussion pertains to a general coupled system with N disciplines. We make a distinction between the *local* design variables (x) that only affect one discipline and the *global* or *shared* design variables (z) that affect more than one discipline. We also need to consider the *coupling* variables (y) that are exchanged between disciplines. Both x and y are discipline specific, and the coupling variables for the ith discipline can be written as,

$$y_i = y_i\left(x_i, y_j, z\right), \tag{1}$$

where $j = 1, \ldots, i-1, i+1, \ldots, N$ is the set of indices that corresponds to the disciplines that the ith discipline depends on, and therefore $j \neq i$. It should be noted that, for purposes of the current discussion, the boldfaced notation that will typically be used in this paper to indicate vector quantities has been temporarily replaced with index notation. When a variable such as x is written without subscript, it represents a vector of all concatenated x_i.

The idea behind the asymmetric suboptimization architecture is that, for certain problems, it may be advantageous to divide the system into two types of disciplines: analysis-only disciplines N_a and disciplines that perform an optimization N_o. Careful consideration is required when designating the disciplines, because only the analyses that are less computationally involved, or those that have many local constraints, are suitable as suboptimization disciplines. In the new formulation, both sets of disciplines are coupled together in the MDA, and all participating disciplines are included so that $N_\mathrm{a} + N_\mathrm{o} = N$.

The system-level optimization problem can be stated as,

$$\begin{aligned} \text{minimize} \quad & F(z, x, y) \\ \text{w.r.t.} \quad & z, x_{a_i} \\ \text{s.t.} \quad & c_{a_i}\left(z, x_{a_i}, y_i\right) \geq 0 \qquad i = 1, \ldots, N_\mathrm{a} \end{aligned} \tag{2}$$

where x_{a_i} and c_{a_i} are the local design variables and constraints of the ith analysis-only discipline. Therefore, the system-level problem is given control over all of the local design variables x_a and constraints c_a of the analysis-only disciplines. The system-level optimizer also varies the design variables that affect more than one discipline, z. The objective function that models the coupled nature of the system is designated as F.

The MDA module contains all of the N_a and N_o disciplines. For a given set of design variables and coupling variable inputs, each analysis-only discipline must satisfy their own governing equations. For the ith discipline, this can be written as,

$$\begin{aligned} \text{given} \quad & z, x_{a_i}, y_j \\ \text{solve} \quad & \mathcal{R}_i\left(z, x_{a_i}, y_j\right) = 0 \\ \text{to get} \quad & y_i. \end{aligned} \tag{3}$$

In other words, the analysis-only discipline generates a set of solutions to satisfy $\mathcal{R}_i$ using the global and local design variables and any required non-local coupling variables.

Each call to a subspace optimization discipline requires not only a solution of the discipline's governing equations, but also an optimization using the local design variables. The subspace optimization problem for the ith discipline can be stated as,

$$\begin{aligned} \text{given} \quad & z, y_j \\ \text{minimize} \quad & F(z, x, y) \\ \text{w.r.t.} \quad & x_{o_i} \\ \text{s.t.} \quad & c_{o_i}\left(z, x_{o_i}, y_i\right) \geq 0 \\ \text{with} \quad & \mathcal{R}_i\left(z, x_{o_i}, y_j\right) = 0 \\ \text{to get} \quad & x_{o_i}, y_i \end{aligned} \tag{4}$$

where x_{o_i} and c_{o_i} are the local design variables and constraints of the ith suboptimization discipline.

The steps involved in the convergence process of the proposed MDO approach closely resemble an MDF procedure (Cramer et al. 1994). Initial values are chosen for all of the global and local design variables. The system-level optimizer passes the z and x_a values into the MDA module, containing all of the discipline analyses. A block-iterative procedure is used to converge the contributing disciplines, keeping in mind that each evaluation of an N_o discipline requires a separate optimization. The MDA is considered to be converged once the coupling variables generated by each discipline analysis have remained constant to within a specified tolerance, over successive iterations. This convergence criteria can be stated mathematically as,

$$y_i^{m+1} = y_i^m \pm \epsilon \qquad i = 1, \ldots, N \tag{5}$$

where y_i^m represents the value of the ith discipline's coupling variables after m iterations, and ϵ is the desired convergence tolerance.

Once the MDA has converged, the derivatives required by the system-level optimizer are calculated. These include the total derivatives of the objective function and system-level constraints with respect to the analysis-only design variables, $\mathrm{d}F/\mathrm{d}x_a$ and $\mathrm{d}c_a/\mathrm{d}x_a$. These derivatives can be efficiently calculated using the method of coupled post-optimality sensitivities (CPOS), which is introduced in Section 2. Once the sensitivities have been computed, they are passed to the system-level optimizer, along with the F and c_a values, which uses the information to determine the next appropriate design step. Subsequently, the updated z and x_a values are returned to the MDA module, and the process is repeated until the system-level optimizer concludes that it has reached the best possible design.

1.4 Aero-structural model

All of our work to date has focused on lower-fidelity aero-structural optimization, which has proven useful in implementing the new architecture and sensitivity method. The aerodynamic analysis employs an inviscid panel code to model the wing, which solves the system,

$$\boldsymbol{A\Gamma} - \boldsymbol{v} = \boldsymbol{0}, \tag{6}$$

where $\boldsymbol{A}$ is the aerodynamic influence coefficients matrix, $\boldsymbol{\Gamma}$ is the vector of panel circulations, and $\boldsymbol{v}$ is the vector of panel boundary conditions, which is simply the local angle of attack of each panel. As indicated by (6), the aerodynamic analysis is being approximated as a linear system. This is not consistent with the motivation behind the new architecture, which is to reduce the number of evaluations of a computationally expensive aerodynamic solver. However, this is taken into account when discussing the results in Section 3.

The aerodynamic discipline also enforces that the wing must produce the lift needed to maintain level flight, i.e.,

$$L - W = 0, \tag{7}$$

where L is the total wing lift and W is the total weight of the aircraft.

The structural model consists of a single wing spar, which is modeled using frame finite elements to represent a tube-shaped spar. The structural analysis is governed by the following equation,

$$\boldsymbol{Ku} - \boldsymbol{f} = \boldsymbol{0}, \tag{8}$$

where $\boldsymbol{K}$ is the stiffness matrix of the structure, $\boldsymbol{u}$ is the displacement vector, and $\boldsymbol{f}$ is the vector of external forces.

The Breguet range equation was selected to provide the objective function. This expression represents the trade-off between the drag and the structural weight of the aircraft, and can be written as,

$$R = \frac{V}{c}\frac{L}{D}\ln\frac{W_i}{W_f}, \tag{9}$$

where V is the cruise velocity, c is the specific fuel consumption, L/D is the ratio of lift to drag, and W_i and W_f are the initial and final weights of the aircraft. The initial weight of the aircraft consists of the structural weight and a fixed fuel weight, whereas the final weight is simply the structural weight. The design variables that we use herein are the jig twist distribution of the wing ($\boldsymbol{\gamma}_{\text{jig}}$), the wall thicknesses of the tube finite elements ($\boldsymbol{t}$), and the wing sweep (Λ).

2 Coupled post-optimality sensitivities (CPOS)

Sensitivity analysis is an important consideration when performing gradient-based optimization, as the derivative calculations are often the most costly step within the optimization cycle. Due to the presence of the structural optimization routine, the new architecture seemed like a logical application of post-optimality sensitivity analysis. Standard post-optimality analysis allows for the change in the optimum solution with respect to a change in a previously fixed parameter to be attained, without having to perform a re-optimization (Braun et al. 1993). Unfortunately, this method does not take into account the coupled nature of the aero-structural system at hand, and it became clear that an extension of the current theory was needed for this work.

The sensitivities of coupled systems can be computed using semi-analytical methods, such as the coupled direct sensitivity equations introduced by Sobieszczanski-Sobieski (1990) or the coupled adjoint method (Martins et al. 2005). These methods allow for the system-level derivatives to be computed without having to resolve the MDA, which greatly reduces the cost and inaccuracy of finite-differencing performed on the entire system analysis. For the aero-structural system involving the coupled aerodynamic residuals ($\boldsymbol{\mathcal{A}}$) and structural residuals ($\mathcal{S}$), as well as the aerodynamic state variables ($\boldsymbol{w}$) and the structural state variables ($\boldsymbol{u}$), the *coupled adjoint equations* can be written as,

$$\begin{bmatrix} \frac{\partial \mathcal{A}}{\partial \boldsymbol{w}} & \frac{\partial \mathcal{A}}{\partial \boldsymbol{u}} \\ \frac{\partial \mathcal{S}}{\partial \boldsymbol{w}} & \frac{\partial \mathcal{S}}{\partial \boldsymbol{u}} \end{bmatrix}^T \begin{bmatrix} \boldsymbol{\psi} \\ \boldsymbol{\phi} \end{bmatrix} = - \begin{bmatrix} \frac{\partial F}{\partial \boldsymbol{w}}^T \\ \frac{\partial F}{\partial \boldsymbol{u}}^T \end{bmatrix}, \tag{10}$$

where $\boldsymbol{\psi}$ and $\boldsymbol{\phi}$ are the aerodynamic and structural adjoint vectors, respectively. The solution of these adjoint equations can then be substituted into the *total sensitivity equation*,

$$\frac{\mathrm{d}F}{\mathrm{d}\boldsymbol{x}} = \frac{\partial F}{\partial \boldsymbol{x}} + \boldsymbol{\psi}^T \frac{\partial \mathcal{A}}{\partial \boldsymbol{x}} + \boldsymbol{\phi}^T \frac{\partial \mathcal{S}}{\partial \boldsymbol{x}}, \tag{11}$$

to find the total derivative of the system-level objective function, F, with respect to the system-level design variables, $\boldsymbol{x}$.

In this context, partial derivatives do not take into account the implicit dependence due to the solution of governing equations, whereas total derivatives do include this implicit dependence.

2.1 Aerodynamic residuals

The aerodynamic and structural residuals are easily identified. As the aerodynamic analysis involves solving (6) and (7), the aerodynamic residuals are the system of equations that result from solving those two equations simultaneously, and can be written as,

$$\mathcal{A} = \begin{bmatrix} \boldsymbol{A} & -\boldsymbol{e} \\ \boldsymbol{e}^T & 0 \end{bmatrix} \begin{bmatrix} \boldsymbol{\Gamma} \\ \alpha \end{bmatrix} - \begin{bmatrix} \boldsymbol{\gamma}_{\text{jig}} + \boldsymbol{\gamma}_{\Delta} \\ nW/qb^2 \end{bmatrix} = \boldsymbol{0}. \tag{12}$$

The local incidence for each panel has been replaced by the individual contributions of jig twist, twist deflection and angle of attack, i.e., $\boldsymbol{v} = -\left(\boldsymbol{\gamma}_{\text{jig}} + \boldsymbol{\gamma}_{\Delta} + \alpha \boldsymbol{e}\right)$, where $\boldsymbol{e}$ is a vector of ones. The second row is a scalar equation that represents the lift constraint (7), where n is the number of panels, q is the free stream dynamic pressure, and b is the wing span. The state variables for the aerodynamic residuals are $\boldsymbol{w}^T = \begin{bmatrix} \boldsymbol{\Gamma}^T & \alpha \end{bmatrix}$, where α is the angle of attack of the aircraft in radians.

2.2 Structural residuals

The structural residuals are given simply by (8), i.e.,

$$\mathcal{S} = \boldsymbol{K}\boldsymbol{u} - \boldsymbol{f} = \boldsymbol{0}. \tag{13}$$

The state variables for the structural residuals are the displacements, $\boldsymbol{u}$. For the MDF architecture, the coupled sensitivities from (12) and (13) can be computed to provide gradients to a single optimization problem. However, for the asymmetric suboptimization architecture, the structural discipline within the MDA module not only involves an analysis, but also a full optimization that must be taken into account when formulating the residual equations.

2.3 Structural optimization residuals

The structural optimization is performed to maximize the aircraft range by varying the internal wing thicknesses, for a given load distribution. The optimization is constrained to prevent the structural stresses ($\boldsymbol{\sigma}$) from exceeding the yield stress of the material and to keep the thicknesses between a minimum gauge value and the radius of the spar and can be stated as,

$$\begin{aligned} \text{maximize} \quad & R \\ \text{w.r.t.} \quad & \boldsymbol{t} \\ \text{s.t.} \quad & \boldsymbol{\sigma}_{\text{yield}} - \boldsymbol{\sigma}\left(\boldsymbol{u}\right) \geq \boldsymbol{0} \\ & \boldsymbol{t} - \boldsymbol{t}_{\min} \geq \boldsymbol{0} \\ & \boldsymbol{r} - \boldsymbol{t} \geq \boldsymbol{0}. \end{aligned} \tag{14}$$

As the structural optimization is a constrained, gradient-based problem, the optimizer is working to satisfy the Karush–Kuhn–Tucker (KKT) conditions. The KKT conditions are necessarily satisfied at a structural optimum, but they do not entirely describe the suboptimization, because an optimum must also be a structural solution. Therefore, combining the structural residuals (13) with the KKT conditions completes the picture and allows us to fully represent the structural optimization residuals:

$$\mathcal{O} = \begin{cases} \boldsymbol{K}\boldsymbol{u} - \boldsymbol{f} & \equiv \mathcal{O}_{\mathcal{S}} \\ \frac{\mathrm{d}R}{\mathrm{d}\boldsymbol{t}} - \boldsymbol{\lambda}_{\sigma}^T \frac{\mathrm{d}\boldsymbol{\sigma}}{\mathrm{d}\boldsymbol{t}} + \boldsymbol{\lambda}_t^T \boldsymbol{I} = \boldsymbol{0} & \equiv \mathcal{O}_{\mathcal{L}} \\ \boldsymbol{\sigma}_{\text{yield}} - \boldsymbol{\sigma} - \boldsymbol{s}_{\sigma}^2 = \boldsymbol{0} & \equiv \mathcal{O}_{\sigma} \\ \boldsymbol{t} - \boldsymbol{t}_{\min} - \boldsymbol{s}_t^2 = \boldsymbol{0} & \equiv \mathcal{O}_t \\ \boldsymbol{s}_{\sigma}\boldsymbol{\lambda}_{\sigma} = \boldsymbol{0}, \quad \boldsymbol{s}_t\boldsymbol{\lambda}_t = \boldsymbol{0} & \equiv \mathcal{O}_{s\lambda} \end{cases} \tag{15}$$

where $\boldsymbol{\lambda}^T = \begin{bmatrix} \boldsymbol{\lambda}_{\sigma}^T & \boldsymbol{\lambda}_t^T \end{bmatrix}$ are the Lagrange multipliers for the stress and thickness constraints, respectively, and $\boldsymbol{s}^T = \begin{bmatrix} \boldsymbol{s}_{\sigma}^T & \boldsymbol{s}_t^T \end{bmatrix}$ are the slack variables associated with those constraints. The radius constraints are omitted from the KKT equations because, although they are used to guide the optimizer away from nonphysical solutions, they are not active at the optimum. Total derivatives are present in the first KKT condition, denoted as $\mathcal{O}_{\mathcal{L}}$ in the optimization residuals (15), because finding the desired sensitivities with respect to the thickness design variables requires the solution of the structural equations. This will be discussed in more detail shortly. The complete set of optimization state variables consists of four vectors, and thus $\boldsymbol{y}^T = \begin{bmatrix} \boldsymbol{u}^T & \boldsymbol{t}^T & \boldsymbol{s}^T & \boldsymbol{\lambda}^T \end{bmatrix}$.

The multidisciplinary analysis of the asymmetric suboptimization method can be viewed as containing two separate disciplines: the aerodynamics and the structural optimization. Having identified the structural optimization residuals, $\mathcal{O}$, we are now able to present the corresponding coupled adjoint equations as,

$$\begin{bmatrix} \frac{\partial \mathcal{A}}{\partial \boldsymbol{w}} & \frac{\partial \mathcal{A}}{\partial \boldsymbol{y}} \\ \frac{\partial \mathcal{O}}{\partial \boldsymbol{w}} & \frac{\partial \mathcal{O}}{\partial \boldsymbol{y}} \end{bmatrix}^T \begin{bmatrix} \boldsymbol{\psi} \\ \boldsymbol{\zeta} \end{bmatrix} = - \begin{bmatrix} \frac{\partial F}{\partial \boldsymbol{w}}^T \\ \frac{\partial F}{\partial \boldsymbol{y}}^T \end{bmatrix}, \tag{16}$$

where $\boldsymbol{\zeta}$ is the adjoint vector associated with the structural subspace optimization. The corresponding total sensitivity is,

$$\frac{\mathrm{d}F}{\mathrm{d}\boldsymbol{x}} = \frac{\partial F}{\partial \boldsymbol{x}} + \boldsymbol{\psi}^T \frac{\partial \mathcal{A}}{\partial \boldsymbol{x}} + \boldsymbol{\zeta}^T \frac{\partial \mathcal{O}}{\partial \boldsymbol{x}}. \tag{17}$$

Recall that the system-level design variables ($\boldsymbol{x}$) for the proposed architecture are the jig twists of each panel ($\boldsymbol{\gamma}_{\mathrm{jig}}$) and the sweep ($\Lambda$), whereas for the MDF method, they include the structural thicknesses ($\boldsymbol{t}$) as well.

Another valid approach to computing the system-level sensitivities for the new architecture is the corresponding coupled direct sensitivity equations. The direct and adjoint methods both involve the exact same partial derivative terms, but the order of operations is different. As a result, the cost of computing the sensitivities using the direct method is practically independent of the number of functions of interest, whereas the cost associated with the adjoint method is essentially independent of the number of design variables. As the new architecture removes the structural constraints from the system-level optimizer, the only function that requires total derivatives is the range equation. Thus, the use of the adjoint CPOS method is particularly advantageous in the asymmetric suboptimization method.

We will now describe the partial derivative terms of the coupled sensitivity equations, both for the MDF method and the new architecture, in more detail.

2.4 Aerodynamic sensitivities

The partial derivative of the aerodynamic residuals with respect to the flow variables can be decomposed as,

$$\frac{\partial \mathcal{A}}{\partial \boldsymbol{w}} = \left[\frac{\partial \mathcal{A}}{\partial \boldsymbol{\Gamma}} \; \frac{\partial \mathcal{A}}{\partial \alpha} \right] = \begin{bmatrix} \boldsymbol{A} & -\boldsymbol{e} \\ \boldsymbol{e}^T & 0 \end{bmatrix}, \tag{18}$$

which is the same matrix shown in (12).

The partial derivative of the aerodynamic residuals with respect to the suboptimization state variables can be broken down as follows,

$$\frac{\partial \mathcal{A}}{\partial \boldsymbol{y}} = \left[\frac{\partial \mathcal{A}}{\partial \boldsymbol{u}} \; \frac{\partial \mathcal{A}}{\partial \boldsymbol{t}} \; \frac{\partial \mathcal{A}}{\partial \boldsymbol{s}} \; \frac{\partial \mathcal{A}}{\partial \boldsymbol{\lambda}} \right] = \begin{bmatrix} -\frac{\partial \boldsymbol{\gamma}_{\Delta}}{\partial \boldsymbol{u}} & \boldsymbol{0} & \boldsymbol{0}\,\boldsymbol{0} \\ 0 & -\frac{n}{qb^2}\frac{\partial W}{\partial \boldsymbol{t}} & 0\;0 \end{bmatrix}, \tag{19}$$

where the only direct effect of the KKT states is the dependence of the weight on the structural thicknesses. Meanwhile, the partial derivatives with respect to the structural state variables involve only the local angle of attack of each panel, which represents how the finite-element displacements are translated into twist deflections.

We write the sensitivities with respect to the system-level design variables as,

$$\frac{\partial \mathcal{A}}{\partial \boldsymbol{x}} = \left[\frac{\partial \mathcal{A}}{\partial \boldsymbol{\gamma}_{\mathrm{jig}}} \; \frac{\partial \mathcal{A}}{\partial \Lambda} \right] = \begin{bmatrix} -\boldsymbol{I} & \frac{\partial \boldsymbol{A}}{\partial \Lambda} \\ \boldsymbol{0} & 0 \end{bmatrix}, \tag{20}$$

where $\boldsymbol{I}$ represents the identity matrix.

The partial derivatives of (19) and (20) were written specifically with the new architecture in mind. However, the MDF sensitivities involve the same terms, but rearranged in a slightly different manner. Instead of being grouped with the KKT variables, $\partial \mathcal{A}/\partial \boldsymbol{u}$ is written on its own, and $\partial \mathcal{A}/\partial \boldsymbol{t}$ is included as a design variable sensitivity. As $\partial \mathcal{A}/\partial \boldsymbol{s}$ and $\partial \mathcal{A}/\partial \boldsymbol{\lambda}$ are both zero, there is fundamentally no difference between the aerodynamic sensitivities required by either architecture.

2.5 Structural analysis sensitivities

The structural equations are included as part of the structural optimization residuals. Therefore, the following sensitivity terms are written explicitly for the MDF method and will be repeated later in the suboptimization sensitivities of the new architecture.

The matrix of sensitivities of the structural residuals with respect to the flow variables involves only the vector of external forces,

$$\frac{\partial \mathcal{S}}{\partial \boldsymbol{w}} = \left[\frac{\partial \mathcal{S}}{\partial \boldsymbol{\Gamma}} \; \frac{\partial \mathcal{S}}{\partial \alpha} \right] = \left[-\frac{\partial \boldsymbol{f}}{\partial \boldsymbol{\Gamma}} \; \boldsymbol{0} \right]. \tag{21}$$

The sensitivity with respect to the structural displacements is simply the stiffness matrix, i.e.,

$$\frac{\partial \mathcal{S}}{\partial \boldsymbol{u}} = \boldsymbol{K}. \tag{22}$$

Finally, the partial derivative of the structural equations with respect to the system-level design variables is,

$$\frac{\partial \mathcal{S}}{\partial \boldsymbol{x}} = \left[\frac{\partial \mathcal{S}}{\partial \boldsymbol{t}}\ \frac{\partial \mathcal{S}}{\partial \boldsymbol{\gamma}_{\mathrm{jig}}}\ \frac{\partial \mathcal{S}}{\partial \Lambda}\right] = \left[\frac{\partial \boldsymbol{K}}{\partial \boldsymbol{t}}\boldsymbol{u}\ \boldsymbol{0}\ \frac{\partial \boldsymbol{K}}{\partial \Lambda}\boldsymbol{u} - \frac{\partial \boldsymbol{f}}{\partial \Lambda}\right], \tag{23}$$

where we note that the jig twists do not directly affect the structure in this case.

2.6 Structural optimization sensitivities

As previously mentioned, the first KKT condition in (15) is written with total derivatives to indicate that it could require solving a set of residual equations. It needs to be clarified that we are only referring to the structural residuals, because the suboptimization operates as a self-contained discipline. As the dependence of the aircraft range on the thickness design variables enters through the structural weight term, and because the weight is only a function of thickness, explicitly or otherwise, it follows that the total derivative of the range with respect to the thicknesses reduces to a partial derivative. Using the chain rule, this can be written as,

$$\frac{\mathrm{d}R}{\mathrm{d}\boldsymbol{t}} = \frac{\partial R}{\partial \boldsymbol{t}} + \underbrace{\frac{\partial R}{\partial \boldsymbol{u}}}_{=0}\frac{\mathrm{d}\boldsymbol{u}}{\mathrm{d}\boldsymbol{t}} = \frac{\partial R}{\partial \boldsymbol{t}}. \tag{24}$$

The thickness constraints are obviously only dependent on the thickness design variables, so the resulting derivatives are nothing more than the identity matrix. However, for the stress constraints, we have,

$$\frac{\mathrm{d}\boldsymbol{\sigma}}{\mathrm{d}\boldsymbol{t}} = \underbrace{\frac{\partial \boldsymbol{\sigma}}{\partial \boldsymbol{t}}}_{=0} + \frac{\partial \boldsymbol{\sigma}}{\partial \boldsymbol{u}}\frac{\mathrm{d}\boldsymbol{u}}{\mathrm{d}\boldsymbol{t}} = \frac{\partial \boldsymbol{\sigma}}{\partial \boldsymbol{u}}\frac{\mathrm{d}\boldsymbol{u}}{\mathrm{d}\boldsymbol{t}}, \tag{25}$$

where the total derivative indicates a need to resolve the structural residuals. Therefore, in terms of the state variables, the $\mathrm{d}\boldsymbol{\sigma}/\mathrm{d}\boldsymbol{t}$ term is dependent on $\boldsymbol{\Gamma}$ and $\boldsymbol{t}$, whereas the stress constraint itself is only a direct function of the displacements.

This information will prove useful when solving the optimization derivatives, because these sensitivities involve second derivatives due to the first KKT condition. For example, the derivatives of the structural optimization residuals with respect to the aerodynamic states are,

$$\frac{\partial \mathcal{O}}{\partial \boldsymbol{w}} = \begin{bmatrix} \frac{\partial \mathcal{O}_{\mathcal{S}}}{\partial \boldsymbol{\Gamma}} & \frac{\partial \mathcal{O}_{\mathcal{S}}}{\partial \alpha} \\ \frac{\partial \mathcal{O}_{\mathcal{L}}}{\partial \boldsymbol{\Gamma}} & \frac{\partial \mathcal{O}_{\mathcal{L}}}{\partial \alpha} \\ \frac{\partial \mathcal{O}_{\sigma}}{\partial \boldsymbol{\Gamma}} & \frac{\partial \mathcal{O}_{\sigma}}{\partial \alpha} \\ \frac{\partial \mathcal{O}_{t}}{\partial \boldsymbol{\Gamma}} & \frac{\partial \mathcal{O}_{t}}{\partial \alpha} \\ \frac{\partial \mathcal{O}_{s\lambda}}{\partial \boldsymbol{\Gamma}} & \frac{\partial \mathcal{O}_{s\lambda}}{\partial \alpha} \end{bmatrix} = \begin{bmatrix} -\frac{\partial \boldsymbol{f}}{\partial \boldsymbol{\Gamma}} & \boldsymbol{0} \\ -\frac{\partial}{\partial \boldsymbol{\Gamma}}\left(\boldsymbol{\lambda}_{\sigma}^{T}\frac{\mathrm{d}\boldsymbol{\sigma}}{\mathrm{d}\boldsymbol{t}}\right) & \boldsymbol{0} \\ \boldsymbol{0} & \boldsymbol{0} \\ \boldsymbol{0} & \boldsymbol{0} \\ \boldsymbol{0} & \boldsymbol{0} \end{bmatrix}, \tag{26}$$

where the higher order dependence of the stress constraints on the flow variables emerges.

The matrix of derivatives of the suboptimization residuals with respect to its own state variables is,

$$\frac{\partial \mathcal{O}}{\partial \boldsymbol{y}} = \begin{bmatrix} \frac{\partial \mathcal{O}_{\mathcal{S}}}{\partial \boldsymbol{u}} & \frac{\partial \mathcal{O}_{\mathcal{S}}}{\partial \boldsymbol{t}} & \frac{\partial \mathcal{O}_{\mathcal{S}}}{\partial \boldsymbol{s}} & \frac{\partial \mathcal{O}_{\mathcal{S}}}{\partial \boldsymbol{\lambda}} \\ \frac{\partial \mathcal{O}_{\mathcal{L}}}{\partial \boldsymbol{u}} & \frac{\partial \mathcal{O}_{\mathcal{L}}}{\partial \boldsymbol{t}} & \frac{\partial \mathcal{O}_{\mathcal{L}}}{\partial \boldsymbol{s}} & \frac{\partial \mathcal{O}_{\mathcal{L}}}{\partial \boldsymbol{\lambda}} \\ \frac{\partial \mathcal{O}_{\sigma}}{\partial \boldsymbol{u}} & \frac{\partial \mathcal{O}_{\sigma}}{\partial \boldsymbol{t}} & \frac{\partial \mathcal{O}_{\sigma}}{\partial \boldsymbol{s}} & \frac{\partial \mathcal{O}_{\sigma}}{\partial \boldsymbol{\lambda}} \\ \frac{\partial \mathcal{O}_{t}}{\partial \boldsymbol{u}} & \frac{\partial \mathcal{O}_{t}}{\partial \boldsymbol{t}} & \frac{\partial \mathcal{O}_{t}}{\partial \boldsymbol{s}} & \frac{\partial \mathcal{O}_{t}}{\partial \boldsymbol{\lambda}} \\ \frac{\partial \mathcal{O}_{s\lambda}}{\partial \boldsymbol{u}} & \frac{\partial \mathcal{O}_{s\lambda}}{\partial \boldsymbol{t}} & \frac{\partial \mathcal{O}_{s\lambda}}{\partial \boldsymbol{s}} & \frac{\partial \mathcal{O}_{s\lambda}}{\partial \boldsymbol{\lambda}} \end{bmatrix}$$
$$= \begin{bmatrix} \boldsymbol{K} & \frac{\partial \boldsymbol{K}}{\partial \boldsymbol{t}}\boldsymbol{u} & \boldsymbol{0} & \boldsymbol{0} \\ \boldsymbol{0} & \frac{\partial^2 R}{\partial \boldsymbol{t}^2} - \frac{\partial}{\partial \boldsymbol{t}}\left(\boldsymbol{\lambda}_{\sigma}^{T}\frac{\mathrm{d}\boldsymbol{\sigma}}{\mathrm{d}\boldsymbol{t}}\right) & \boldsymbol{0} & \left[-\frac{\mathrm{d}\boldsymbol{\sigma}}{\mathrm{d}\boldsymbol{t}}\ \ \boldsymbol{I}\right] \\ -\frac{\partial \boldsymbol{\sigma}}{\partial \boldsymbol{u}} & \boldsymbol{0} & \left[-2\boldsymbol{s}_{\sigma}\ \ \boldsymbol{0}\right] & \boldsymbol{0} \\ \boldsymbol{0} & \boldsymbol{I} & \left[\boldsymbol{0}\ \ -2\boldsymbol{s}_{t}\right] & \boldsymbol{0} \\ \boldsymbol{0} & \boldsymbol{0} & \boldsymbol{\lambda} & \boldsymbol{s} \end{bmatrix}. \tag{27}$$

Once again, we encounter higher-order derivatives, this time due to the second-order dependence of the range and stress constraints on the thicknesses.

Finally, only the sweep design variable has a direct effect on the suboptimization residuals, and thus,

$$\frac{\partial \mathcal{O}}{\partial \boldsymbol{x}} = \begin{bmatrix} \frac{\partial \mathcal{O}_{\mathcal{S}}}{\partial \boldsymbol{\gamma}_{\mathrm{jig}}} & \frac{\partial \mathcal{O}_{\mathcal{S}}}{\partial \Lambda} \\ \frac{\partial \mathcal{O}_{\mathcal{L}}}{\partial \boldsymbol{\gamma}_{\mathrm{jig}}} & \frac{\partial \mathcal{O}_{\mathcal{L}}}{\partial \Lambda} \\ \frac{\partial \mathcal{O}_{\sigma}}{\partial \boldsymbol{\gamma}_{\mathrm{jig}}} & \frac{\partial \mathcal{O}_{\sigma}}{\partial \Lambda} \\ \frac{\partial \mathcal{O}_{t}}{\partial \boldsymbol{\gamma}_{\mathrm{jig}}} & \frac{\partial \mathcal{O}_{t}}{\partial \Lambda} \\ \frac{\partial \mathcal{O}_{s\lambda}}{\partial \boldsymbol{\gamma}_{\mathrm{jig}}} & \frac{\partial \mathcal{O}_{s\lambda}}{\partial \Lambda} \end{bmatrix} = \begin{bmatrix} \boldsymbol{0} & \frac{\partial \boldsymbol{K}}{\partial \Lambda}\boldsymbol{u} - \frac{\partial \boldsymbol{f}}{\partial \Lambda} \\ \boldsymbol{0} & -\frac{\partial}{\partial \Lambda}\left(\boldsymbol{\lambda}_{\sigma}^{T}\frac{\mathrm{d}\boldsymbol{\sigma}}{\mathrm{d}\boldsymbol{t}}\right) \\ \boldsymbol{0} & -\frac{\partial \boldsymbol{\sigma}}{\partial \Lambda} \\ \boldsymbol{0} & \boldsymbol{0} \\ \boldsymbol{0} & \boldsymbol{0} \end{bmatrix}. \tag{28}$$

3 Results and discussion

Before running any MDO trials, the CPOS equations that we developed for the new asymmetric suboptimization method were verified against the finite-difference approach. The two methods are compared in Table 1 for a trial with five jig twist and five thickness design variables, corresponding to five panels and five elements. The jig twist of the first panel was held fixed. The partial derivatives in the CPOS equations are calculated using the complex-step derivative approximation (Squire and Trapp 1998; Martins et al. 2003), which provides numerically exact values.

As shown in Table 1, the CPOS adjoint results agree with finite-differences to five digits. The CPOS results are more accurate due to subtractive cancellation errors in the finite-difference estimates. The main advantage of the CPOS method is clear: The computational time was only 3% of the time required by finite differences. Therefore, the CPOS method accurately models the response of our tightly coupled system, without having to re-converge the analysis or even once re-optimize the subspace problem, which offers significant savings over the finite-difference approach.

To better understand the computational costs involved in the CPOS adjoint, a cost breakdown of computing the total derivatives is shown in Table 2. In this study, both the number of panels and the number of finite elements were increased to 50. It is evident that computing the partial derivatives is by far the costliest step, with most of this expense being attributed to the partial derivatives of the KKT system. This is not surprising, as the subspace optimization derivatives involve the second-order terms in (26), (27), and (28). These higher-order derivatives are currently being calculated by using the complex-step method to determine the first-order derivatives and then performing a finite differencing over the routine to obtain the second-order derivatives.

The reason the calculation of the partial derivative terms outweighs the adjoint solution is because the current aero-structural model is written in the scripting language Python, whereas the adjoint vectors are computed using a linear solve operation in a precompiled numerical package. Most large-scale scientific computing requires the use of a compiled language such as Fortran. When optimization is performed on these higher-fidelity systems, solving the system of equations required by the direct and adjoint methods typically becomes the dominant expense, and the use of the adjoint method becomes more advantageous. As shown in Table 2, increasing the number of design variables from 5 to 50 does not effect the time required to compute the adjoint vectors. The only cost increase is due to the dependence of the aerodynamic residuals on the jig twists.

Table 1 Sensitivity analysis comparison

$\mathrm{d}F/\mathrm{d}\boldsymbol{x}$	Finite-difference	CPOS adjoint
$\mathrm{d}R/\mathrm{d}\gamma_2$	6,725.7012	6,725.7087
$\mathrm{d}R/\mathrm{d}\gamma_3$	3,530.1758	3,530.1016
$\mathrm{d}R/\mathrm{d}\gamma_4$	−2,580.8521	−2,580.8579
$\mathrm{d}R/\mathrm{d}\gamma_5$	−5,198.1801	−5,198.1781
$\mathrm{d}R/\mathrm{d}\Lambda$	−702.2317	−702.2368
Elapsed time (s)	150.50	4.36

Table 2 Computational cost of CPOS adjoint, in seconds

Number of jig twists	5	50
Partial derivatives	282.73	290.52
Aerodynamic	61.51	69.18
Structural	18.19	18.11
Subspace optimization	198.58	198.67
Adjoint solution	0.29	0.29
Compute total sensitivity	<0.01	<0.01
Total time (s)	283.03	290.82

Having validated the CPOS method, we performed optimization using these sensitivities and compared the performance of the asymmetric suboptimization approach against the traditional MDF method. For both the MDF and the CPOS methods, a fixed-point iteration scheme was used to converge the MDA. The corresponding coupled adjoint formulations were used to determine the system-level sensitivities for the two architectures. The MDO trials were performed based on four separate parameters: the number of aerodynamic design variables (N_γ), the number of structural design variables (N_t), the number of aerodynamic panels (N_{panel}), and the number of structural elements (N_{elem}). These four parameters were varied independently to determine the effect that each one had on the architectures being compared. The computations were run on a 1.5 GHz Itanium 2 processor in an SGI Altix with 32 GB RAM, and the results are listed in Table 3.

3.1 Reference trial

Trial 1, with five aerodynamic and five structural design variables, 30 panels and 30 elements, was selected as the reference case. Table 3 shows that, for this case, the MDF architecture required almost three times as many system-level iterations as the new architecture to find the optimum and required an average of three

Table 3 Trials of variable dimensionality comparing the MDF method and the asymmetric suboptimization architecture; times are measured in seconds

Trial	N_γ	N_t	N_{panel}	N_{elem}	Method	MDA evaluations	Avg. MDA iterations per Eval.	Elapsed time	Struct. time	Aero. time	MDA sensitivities time	Required T_A/T_S
1	5	5	30	30	MDF	48	16.38	2,022.57	210.57	51.78	1,757.15	**9.53**
					AS	17	13.47	3,407.47	1,698.89	15.20	1,692.14	
2	5	**10**	30	30	MDF	55	17.47	2,423.28	257.46	63.48	2,098.20	**14.87**
					AS	16	12.75	5,389.54	2,739.04	13.49	2,635.87	
3	5	**15**	30	30	MDF	54	17.30	2,463.01	250.65	61.88	2,145.83	**26.85**
					AS	16	12.63	7,689.64	3,786.63	13.34	3,888.51	
4	**10**	5	30	30	MDF	64	15.91	2723.12	273.12	67.12	2,378.39	**6.31**
					AS	20	13.25	3,949.18	1,944.82	17.37	1,985.52	
5	**15**	5	30	30	MDF	87	15.51	3,723.36	361.13	88.97	3,266.62	**4.09**
					AS	25	12.56	4,789.61	2,274.67	20.58	2,492.53	
6	5	5	30	**60**	MDF	54	18.04	5,905.07	539.09	64.16	5,279.23	**2.22**
					AS	16	12.19	6,809.87	3,080.30	12.84	3,715.55	
7	5	5	30	**90**	MDF	53	16.30	10,782.48	742.01	57.39	9,978.08	**0.68**
					AS	15	11.67	11,136.28	5,035.69	11.59	6,087.87	
8	5	5	**60**	30	MDF	49	16.22	5,244.75	233.91	195.20	4,810.25	**1.27**
					AS	17	12.29	5,319.42	1,624.47	52.23	3,639.52	
9	5	5	**90**	30	MDF	46	17.11	10,361.44	242.90	427.84	9,683.00	**0.73**
					AS	18	11.22	8,346.52	1,510.32	109.72	6,720.16	

more iterations between the aerodynamic and structural disciplines to converge the MDA. The fewer number of calls to the MDA is what we expected from the new method, whose central idea is to nest the structural optimization problem in the MDA and simplify the system-level problem. The system-level optimizer of the new architecture is unconstrained and only in charge of the aerodynamic design variables, whereas the MDF optimizer has the added burden of controlling both the aerodynamic and structural design variables, as well as satisfying the stress and thickness constraints at each element. The fewer number of iterations required within the MDA is another advantage of the asymmetric suboptimization architecture. This occurs because the presence of the structural optimization in the MDA module makes the wing stiffer than it would be otherwise (because the stress constraints need to be satisfied). The stiffer wing limits the displacements, resulting in better convergence of the aero-structural cycle.

The timings of the first trial, listed in Table 3, do not show the true potential of the new architecture. For the reference trial, the new architecture takes almost 1,500 s longer overall than the MDF method. This is largely due to the total time spent performing structural analysis and optimization, which is the consequence of having an optimizer in the MDA module. In addition, the time required to calculate the system-level sensitivities after each MDA solution is greater for the new architecture, due to the second-order terms. However, as shown in Fig. 3, the asymmetric suboptimization method converges to the optimum with fewer evaluations of the coupled system, as compared to the MDF method. With fewer MDA iterations, the new architecture succeeds in reducing the amount of time performing aerodynamics analysis, accomplishing the goal of the proposed formulation.

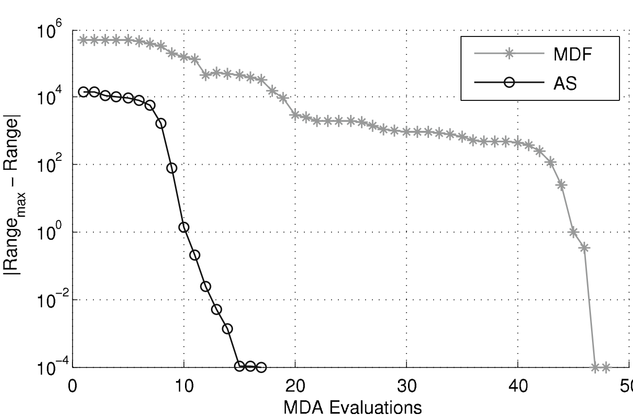

Fig. 3 Range convergence plots for Trial 1

We now derive the performance metric used to evaluate the new approach: the ratio of the aerodynamic solver time to structural solver time required to make the asymmetric suboptimization and MDF cost the same overall. The total time required by MDF can be broken down as follows,

$$T_{\text{total}} = N\left(T_{\text{A}} + T_{\text{S}}\right) + T_{\text{O}}, \tag{29}$$

where N is the total number of aero-structural iterations, T_{A} is the time for an aerodynamic analysis, T_{S} is the time for a structural analysis, and T_{O} represents the overhead, which is the rest of the time and is composed primarily of the time spent computing the MDA sensitivities. Similarly, the total time of the new method can be broken down as,

$$T'_{\text{total}} = N'\left(T_{\text{A}} + T_{\text{SO}}\right) + T'_{\text{O}}, \tag{30}$$

where T_{SO} is the time required for a single structural suboptimization. Equating the two total times and solving for the ratio yields,

$$\frac{T_{\text{A}}}{T_{\text{S}}} = \frac{1}{N' - N}\left[\frac{T_{\text{O}} - T'_{\text{O}}}{T_{\text{S}}} + N - N'\frac{T_{\text{SO}}}{T_{\text{S}}}\right]. \tag{31}$$

This equation expresses the ratio of computational cost between the aerodynamic and structural solvers that is needed for the new method to break even with MDF. A ratio greater than the one calculated using this formula indicates a situation where the new method is the more efficient approach.

For Trial 1, the computed ratio is 9.53 and is shown as the last column in Table 3. These ratios will be used as the main metric during our discussion of the different comparison trials. As higher-fidelity scenarios involve an aerodynamic solution time at least an order of magnitude greater than the structural solution, *a time ratio less than ten is a favorable result for the new architecture*. Certain high-fidelity frameworks might even encounter aerodynamic-to-structural time ratios of up to 10^3, depending on the particular solvers being used.

The effect of independently varying the four parameters (N_t, N_γ, N_{elem}, and N_{panel}) will now be investigated.

3.2 Increasing the number of structural design variables

Trials 2 and 3 in Table 3 show the effect of increasing the number of structural design variables. For the MDF method, the added design variables result in a few additional optimization iterations, which translates into proportional increases in the structural, aerodynamic, and sensitivity analysis times. For the new architecture, the additional structural variables do not change the system-level problem.

The added structural variables complicate the subspace optimization of the new architecture, causing longer structural times. The constraint gradients are the main cause for this delay, because the computational time of the complex-step method scales with the number of design variables. Increasing N_t also slows down the total MDA sensitivity time for the new architecture. The thickness variables act as state variables of the structural optimization residuals, and increasing N_t increases the size of the sensitivity matrices. Subsequently, increasing N_t exhibits an unfavorable trend for the asymmetric suboptimization method, and the required aerodynamic-to-structural time ratio increases significantly.

3.3 Increasing the number of aerodynamic design variables

Trials 4 and 5 in Table 3 show the effect of increasing the number of aerodynamic design variables. Increasing the number of jig twists has a considerable effect on the number of MDF iterations required. The number of system-level iterations of the new architecture increases as well, but not as drastically, due to the absence of constraints.

For both architectures, the structural, aerodynamic, and MDA sensitivity times increase relative to the reference trial. However, this increase is directly proportional to the increase in MDA evaluations, and as a result, the trend favors the new architecture. The required aerodynamic-to-structural time ratio decreases, and a further increase in N_γ would result in the new formulation being more computationally efficient than the MDF approach.

3.4 Increasing the structural model fidelity

Trials 6 and 7 demonstrate what happens with a larger number of structural elements, which increases both the fidelity of the structural analysis and the amount of structural constraints.

For the MDF approach, these added constraints only slightly increase the number of optimizer iterations. These additional states significantly affect the structural subspace optimization. The time required to compute the constraints and their sensitivities increases with the number of elements, because each stress evaluation involves solving the structural residuals. However, the increase in time required to evaluate the MDA sensitivities is the dominating factor. As the MDF method requires over three times as many MDA evaluations as the new architecture, the total time dedicated to calculating the system-level sensitivities is much greater. As a result, the new architecture shows a favorable trend, as shown by the decrease in the required aerodynamic-to-structural ratio.

3.5 Increasing the aerodynamic model fidelity

Finally, Trials 8 and 9, reveal the effect of an increased number of panels and, consequently, an increased number of aerodynamic states ($\boldsymbol{w}$). This leads to a more costly aerodynamic analysis, and Trial 9 is the first MDF trial where the aerodynamic analysis is more expensive to compute than the structural analysis.

The larger aerodynamic state vector also increases the MDA sensitivity times of both architectures, but the total MDF times increase more rapidly due to the higher number of MDA evaluations. Thus, for both Trials 8 and 9, the total MDA sensitivity time is lower for the proposed architecture. As a result, the required aerodynamic-to-structural ratio decreases with increasing panels, and Trial 9 illustrates a situation where the new asymmetric suboptimization method is the faster approach.

3.6 Summary

The different performance comparisons show that the new asymmetric suboptimization method exhibits an unfavorable trend when the number of structural design variables are increased and a favorable trend when the number of aerodynamic design variables or the fidelity of the analyses are increased. This indicates that the new architecture becomes the more efficient approach under two conditions: either when the new formulation adequately reduces the number of MDA evaluations or when there is a large enough discrepancy between disciplinary solution times. In other words, if the simplified system-level problem results in significantly fewer calls to the coupled system, the new architecture is the better approach. Similarly, if the ratio of aerodynamic-to-structural solution times is large enough, the new architecture again becomes the more attractive method. A design problem that involves many constraint-critical design variables and that employs a computationally intensive aerodynamics solver satisfies both conditions and presents an ideal application for the new architecture.

4 Conclusions

We developed a new subspace optimization method for performing aero-structural design that uses a coupled adjoint sensitivity method for determining the required system-level derivatives. We showed that this asymmetric suboptimization approach offers computational advantages when compared to the traditional MDF method: it simplifies the system-level problem, resulting in fewer calls to the MDA module, fewer total iterations, and fewer evaluations of the aerodynamic analysis.

Simple extrapolations of the results demonstrate that the new architecture becomes increasingly attractive, as either the number of aerodynamic design variables or the fidelity of the aero-structural analysis is increased. This was possible due to the sensitivity equations that were developed, which involve including the structural optimization residuals in the coupled adjoint sensitivity equations.

More generally, the adjoint CPOS method developed herein can be applied to any MDO problem and is particularly suited to problems where there are large discrepancies between the computational costs of the disciplinary solvers.

References

Braun RD, Kroo IM, Gage PJ (1993) Post-optimality analysis in aerospace vehicle design. In: Proceedings of the AIAA aircraft design, systems and operations meeting, Monterey. CA, AIAA, pp 93–3932

Braun RD, Gage PJ, Kroo IM, Sobieski IP (1996) Implementation and performance issues in collaborative optimization. AIAA Paper pp 96–4017

Chattopadhyay A, Pagaldipti N (1995) A multidisciplinary optimization using semi-analytical sensitivity analysis procedure and multilevel decomposition. Comput Math Appl 29(7): 55–66

Cramer EJ, Dennis JE, Frank PD, Lewis RM, Shubin GR (1994) Problem formulation for multidisciplinary optimization. SIAM J Optim 4(4):754–776, http://citeseer.nj.nec.com/article/cramer93problem.html

Giunta AA (2000) A novel sensitivity analysis method for high fidelity multidisciplinary optimization of aero-structural systems. AIAA Paper 2000–0683

Kodiyalam S, Sobieszczanski-Sobieski J (2002) Bilevel integrated system synthesis with response surfaces. AIAA J 38(8): 1479–1485

Kroo IM (1997) MDO for large-scale design. In: Multidisciplinary design optimization: state-of-the-art, SIAM, Philadelphia

Martins JRRA, Alonso JJ, Reuther JJ (2004) High-fidelity aerostructural design optimization of a supersonic business jet. J Aircr 41(3):523–530

Martins JRRA, Alonso JJ, Reuther JJ (2005) A coupled-adjoint sensitivity analysis method for high-fidelity aero-structural design. Optim Eng 6(1):33–62, http://www.kluweronline.com/issn/1389-4420/contents

Martins JRRA, Sturdza P, Alonso JJ (2003) The complex-step derivative approximation. ACM Trans Math Softw 29(3):245–262, http://doi.acm.org/10.1145/838250.838251

Maute K, Nikbay M, Farhat C (2001) Coupled analytical sensitivity analysis and optimization of three-dimensional nonlinear aeroelastic systems. AIAA J 39(11):2051–2061

Poon NMK, Martins JRRA (2007) An adaptive approach to constraint aggregation using adjoint sensitivity analysis. Struct Multidisc Optim 30(1):61–73

Sobieski IP, Kroo IM (2000) Collaborative optimization using response surface estimation. AIAA J 38(10):1931–1938

Sobieszczanski-Sobieski J (1990) Sensitivity of complex, internally coupled systems. AIAA J 28(1):153–160

Sobieszczanski-Sobieski J, Haftka RT (1997) Multidisciplinary aerospace design optimization: survey of recent developments. Struct Optim 14(1):1–23

Sobieszczanski-Sobieski J, Agte JS, Robert R, Sandusky J (1998) Bi-level integrated system synthesis (BLISS). AIAA Paper 98–4916

Squire W, Trapp G (1998) Using complex variables to estimate derivatives of real functions. SIAM Rev 40(1):110–112, http://epubs.siam.org/sam-bin/dbq/article/31241

Tedford NP, Martins JRRA (2006) On the common structure of MDO problems: a comparison of architectures. In: Proceedings of the 11th AIAA/ISSMO multidisciplinary analysis and optimization conference, Portsmouth, VA, AIAA 2006-7080

Tribes C, Dube JF, Trépanier JY (2005) Decomposition of multidisciplinary optimization problems: formulations and application to a simplified wing design. Eng Optim 37(8): 775–796